HHS Public Access

Author manuscript

Neuropathology. Author manuscript; available in PMC 2017 June 05.

Published in final edited form as:

Neuropathology. 2016 April ; 36(2): 146–156. doi:10.1111/neup.12242.

ACTIVATION OF EXTRACELLULAR REGULATED KINASE AND MECHANISTIC TARGET OF RAPAMYCIN PATHWAY IN FOCAL CORTICAL DYSPLASIA

Vinit V. Patil[1,8,9,10], **Miguel Guzman**[10], **Angela N. Carter**[5,8,9], **Geetanjali Rathore**[6], **Daniel Yoshor**[4], **Daniel Curry**[4], **Angus Wilfong**[2,6], **Satish Agadi**[2,6], **John W. Swann**[1,5,6,8,9], **Adekunle M. Adesina**[3], **Meenakshi B. Bhattacharjee**[7], and **Anne E. Anderson**[1,2,5,6,8,9]

[1]Program in Translational Biology and Molecular Medicine at Baylor College of Medicine, Houston, Texas, USA

[2]Department of Neurology at Baylor College of Medicine, Houston, Texas, USA

[3]Department of Pathology at Baylor College of Medicine, Houston, Texas, USA

[4]Department of Neurosurgery at Baylor College of Medicine, Houston, Texas, USA

[5]Department of Neuroscience at Baylor College of Medicine, Houston, Texas, USA

[6]Department of Pediatrics at Baylor College of Medicine, Houston, Texas, USA

[7]Department of Pathology and Laboratory Medicine, University of Texas Medical School, Houston, Texas, USA

[8]Cain Foundation Laboratories at Texas Children's Hospital, Houston, Texas, USA

[9]Jan and Dan Duncan Neurological Research Institute at Texas Children's Hospital, Houston, Texas, USA

[10]Department of Pathology, Saint Louis University, Saint Louis, Missouri

Abstract

Neuropathology of resected brain tissue has revealed an association of focal cortical dysplasia (FCD) with drug resistant epilepsy (DRE). Recent studies have shown that the mechanistic target of rapamycin (mTOR) pathway is hyperactivated in FCD as evidenced by increased phosphorylation of the ribosomal protein S6 (S6) at serine 240/244 ($S^{240/244}$), a downstream target of mTOR. Moreover, extracellular regulated kinase (ERK) has been shown to phosphorylate S6 at serine 235/236 ($S^{235/236}$) and tuberous sclerosis complex 2 (TSC2) at serine 664 (S^{664}) leading to hyperactive mTOR signaling. We evaluated ERK phosphorylation of S6 and TSC2 in two types of FCD (FCD I and FCDII) as a candidate mechanism contributing to mTOR pathway dysregulation in this disorder. Tissue samples from patients with tuberous sclerosis (TS) served as a positive control. Immunostaining for phospho-S6 ($pS6^{240/244}$ and $pS6^{235/236}$), phospho-ERK (pERK), and phospho-TSC2 (pTSC2) was performed on resected brain tissue with FCD and TS. We found increased $pS6^{240/244}$ and $pS6^{235/236}$ staining in FCD I, FCD II, and TS compared to normal

Corresponding author: Dr. Anne Anderson, Jan and Dan Duncan Neurological Research Institute, Texas Children's Hospital, 1250 Moursund Street, Suite 1225, Houston, Texas 77030, Telephone: 832-824-3976, Fax: 832-825-1248, annea@bcm.edu.

appearing tissue, while pERK and pTSC2 staining was increased only in FCD IIb and TS tissue. Our results suggest that both the ERK and mTOR pathways are dysregulated in FCD and TS; however, the signaling alterations are different for FCD I as compared to FCD II and TS.

Keywords

focal cortical dysplasia (FCD); tuberous sclerosis (TS); drug resistant epilepsy (DRE); mechanistic target of rapamycin (mTOR); extracellular-regulated kinase (ERK)

INTRODUCTION

Focal cortical dysplasia (FCD) is a malformation of cortical development that is associated with a spectrum of clinical disorders such as tuberous sclerosis (TS), hemimegalencephaly, and gangliogliomas (1–4). Additionally, FCD has variable clinical features ranging from drug-resistant epilepsy (DRE) to cognitive and behavioral deficits including autism spectrum disorders (5). FCD is classified into FCD I, FCD IIa, FCD IIb and FCD III depending on the types of cortical layering defects, the presence of normal-sized versus abnormally large dysmorphic neurons, and the association of secondary lesions such as hippocampal sclerosis or ganglioglioma (4, 6, 7). It has been suggested recently that somatic mutations contribute to the etiology of FCD (3, 4, 8–12). However, little is known about the molecular mechanisms that contribute to the pathology underlying FCD. Interestingly, FCD shares common pathologic and molecular phenotypes with TS, which is characterized by mutations in tuberous sclerosis complex 1 or 2 (*TSC1/2*) and activation of the mechanistic target of rapamycin (mTOR) pathway (13–15). Increased mTOR signaling has been shown in large dysmorphic neurons and balloon cells from FCD IIb (16).

mTOR is a serine/threonine kinase which regulates cellular growth (17, 18). In the nervous system, mTOR signaling functions include modulation of inhibitory synapses onto excitatory neurons (19), synaptic plasticity (20), gliogenesis (21), autophagy (22), and Tau protein homeostasis (23). Additionally, mTOR regulates cell placement and morphogenesis (24–27), which are abnormal in FCD. The mTOR pathway is highly regulated and TSC1/2 proteins negatively regulate the activation of the mechanistic target of rapamycin complex 1 (mTORC1) (28–30). mTORC1 is a protein complex formed by the mTOR kinase and number of associated molecules, which indirectly regulates phosphorylation of downstream effector molecules involved in the translational machinery, such as ribosomal protein S6 (S6) (31–33). Mutations in *TSC1* or *TSC2* lead to the dissociation of the TSC1/2 complex and loss of the negative regulatory function on mTORC1 resulting in increased phosphorylation of S6 as seen in TS (34).

Phosphorylation of S6 has been considered a surrogate marker of mTORC1 pathway activation as S6 can be phosphorylated at serine 240/244 ($S^{240/244}$) and serine 235/236 ($S^{235/236}$) via S6 kinase I (S6K1), which is activated by mTORC1 (35). However, activated extracellular regulated kinase (ERK) (36, 37) can also phosphorylate S6 at $S^{235/236}$ (35). Moreover, ERK phosphorylates TSC2 leading to TSC1/2 complex dissociation and loss of negative regulation of mTORC1 with increased phosphorylation of S6 (30, 38). In addition to phosphorylating TSC2 and S6, ERK can directly influence mRNA transcription and

protein synthesis and regulate cell growth (39, 40) and synaptic plasticity (41). Interestingly, increased ERK phosphorylation in EMX-Cre TSC1 conditional knockout mice, a model of TS with cortical dysplasia and seizures has also been demonstrated (42).

Govindrajan et al. (43) and Jozwiak et al. (44) found increased levels of ERK phosphorylation in tubers from TS patients compared to control brain tissue obtained from epilepsy surgery patients. While the dysplastic tissue in TS shows upregulated ERK signaling, the activation status of ERK in dysplastic tissue in FCD is unknown. Thus, we hypothesized that both ERK and mTOR signaling are altered in FCD. We utilized immunohistochemistry to evaluate the phosphorylation status of ERK, TSC2, and S6 in FCD tissue samples obtained from epilepsy surgical resections to further characterize mTOR signaling in this disorder.

MATERIALS AND METHODS

Human tissue specimens

Resected brain tissue was obtained from individuals with DRE who underwent epilepsy surgery at the Texas Children's Hospital (Houston, TX). The amount of tissue available for neuropathology was variable depending on the extent of the lesion, ictal onset zone, and eloquent cortex. This was a clinical determination made by the neurosurgeon and epileptologist. The tissue and clinical history were obtained after consenting patients according to The Institutional Review Board protocol approved by Baylor College of Medicine.

Clinical features and Magnetic Resonance Imaging

Demographics and clinical features that included the location of the epileptic focus, associated medical conditions, surgical outcome, MRI findings, and the neuropathology reports were obtained from the patient medical records. Patients who had seizures secondary to a primary lesion such as dysembryoplastic neuroepithelial tumor, vascular malformation, or ganglioglioma were also included in the study as epilepsy controls. Surgical outcome was scored according to Engel's classification (45). Briefly, this classification consists of four classes that are ranked based on seizure freedom or improvement. Engel Class 1 outcome includes individuals completely free from disabling seizures. Class 2 includes individuals with rare disabling seizures. Class 3 includes individuals with prolonged seizure-free intervals amounting to half the follow-up period but not less than two years. Class 4 includes individuals without any worthwhile improvement in seizures.

Histology

The tissue specimens were evaluated by the clinical neuropathology service. We obtained 5–7 sections for hematoxylin and eosin (H&E), immunostaining, and antibody controls from the available tissue blocks from each case. Two neuropathologists (MBB and AMA) reviewed these sections to confirm sequential sections and the type of FCD as well as staining for various mTOR and ERK markers. These stained sections were scored for immunoreactivity by a neuropathologist blind to the clinical history. H&E staining was performed on 5 μm sections to histologically identify the types of cortical dysplasia (Table

1). Sections were deparaffinized in four washes of xylene for 5 minutes each, rehydrated in four washes of 100% ethanol for 5 minutes \and then stained with H&E according to manufacturer's protocol (Sigma-Aldrich, St. Louis MO). Stained sections were dehydrated by washing in an increasing ethanol gradient (75– 100%) followed by 4 washes of xylene. After dehydration, sections were mounted in cytoseal 60 mounting media (Richard Allen Scientific, Rockford, IL). The normal appearing neurons present on the sections with FCD or tumors were used as negative controls (Fig. 1). Dysplastic tissue obtained from individuals with TS, which is known to have pathological mTOR pathway activation (37, 46–49), was included as a positive control.

Immunohistochemistry

Immunohistochemistry (IHC) was performed as previously described (50). Briefly, the tissue was fixed in 10% formalin, embedded in paraffin, cut into 5 μm sections, and mounted on pre-cleaned Superfrost plus slides (VWR International, West Chester, PA). One section from each specimen was stained with H&E, and adjacent sections were immunostained with antibodies against phospho-S6 (pS6) at the serine 240/244 ($S^{240/224}$)- and at the serine 235/236 ($S^{235/236}$) sites (rabbit anti-$pS6^{240/244}$ 1:200, rabbit anti-$pS6^{235/236}$ 1:200, Cell Signaling Technology), phospho-ERK (pERK) at the tyrosine 202 (Y^{202}) and threonine 204 (T^{204}) sites (rabbit anti-pERK; 1:200, Cell Signaling Technology), and phospho-TSC2 (pTSC2) at the serine 664 (S^{664}) site (rabbit anti-pTSC2; 1:50, Biolegend, San Diego, CA). A total of 1–2 sections per individual were stained with each antibody. Sections were incubated with the primary antibodies for 24 hours at 4°C, followed by three washes in phosphate buffered saline (PBS; 137 mM NaCl, 2.7 mM KCl, 4.3 mM Na_2HPO_4, 1.47 mM KH_2PO_4, pH 7.4) with 0.1% Triton (1X PBS-T) for 10 minutes each. The sections were then incubated in biotin-labeled secondary antibody (goat anti-rabbit; 1:200; Cell Signaling Technology) for 2 hours. Following incubation with goat anti-rabbit secondary antibody, sections were washed three times in 1X PBS and then incubated in peroxidase-conjugated avidin (Vectastain Elite ABC kit, Burlingame, CA) for 45 minutes at room temperature. The antigen-antibody complex was detected by the Nova RED kit (Vector Laboratories). Stained sections were then counterstained with hematoxylin (Sigma-Aldrich), dehydrated in increasing ethanol concentrations, cleared in xylene, and prepared for viewing using cytoseal 60 mounting medium (Thermo Scientific, Rockford, IL). Microscopy was performed using an Olympus BX51 microscope equipped with either an Olympus DP70 or a Nikon Eclipse Ti color digital camera. The intensity and distribution of positive staining was evaluated using an IHC score obtained by multiplying the intensity grade (scale 0 to 3) by the percentage of positively-stained dysplastic brain parenchyma. Each case was graded by two independent pathologists (VVP and MAG) as follows: 0 = no staining, 1 = weak staining, 2 = intermediate staining, and 3 = strong staining. The percentage of the positive-stained dysplastic brain was assessed on a low power magnification (4X) by the same examiners. Statistical significance for IHC score amongst FCD I, FCD IIa, FCD IIb and TS was analyzed using One-way ANOVA with Tukey's post hoc test.

RESULTS

The tissue was classified according to the type of FCD and the clinical features of each individual were used to identify potential pathophysiological associations. Markers for activation of the mTOR and ERK pathways in different types of available FCD tissue were evaluated using immunohistochemical staining with phospho-selective antibodies.

Identification of different types of FCD in the resected tissue

Using the International League Against Epilepsy (ILAE) 2011 classification (52), the twenty-one patients analyzed were as follows: FCD I (n=8), FCD IIa (n=3), FCD IIb (n=4), TS (n=2), and the remaining patients were epilepsy controls (n=4; Table 1). The non-dysplastic tissue with normal appearing neurons (Figure 1A, F) from patients who underwent brain resection for causes other than FCD was used as an epilepsy control. Dysmorphic neurons, which were identified by abnormal shape and orientation, were present in all three types of FCD. FCD I tissue had normal-sized dysmorphic neurons (< 20 μm in diameter) arranged in columns instead of the normal cortical laminar pattern (Figure 1B -). The large dysmorphic neurons (> 20 μm in diameter) were found in FCD IIa (Figure 1C, H), FCD IIb (Figure 1D, I) and TS (Figure 1E, K). Large polygonal cells with pale eosinophilic cytoplasm and eccentric nuclei were classified as balloon cells. Balloon cells were found in the white matter and large dysmorphic neurons were located in the cortex and white matter from FCD IIb tissue (Figure 1D, J). TS tissue was characterized by the presence of giant cells, which were similar to balloon cells in addition to normal-sized and large dysmorphic neurons (Figure 1E,).

Demographics, Clinical Features, and Magnetic Resonance Imaging

As shown in Table 1, the age of the patients included in this study ranged from 5 months to 18 years, with the age of seizure onset between 0.42 – 10.5 years. As previously described by Kim et al.(53), MRI lesions were most commonly associated with FCD II (Table 1). In the tissue we evaluated, MRI lesions were present in two cases of FCD I, while MRI lesions were present in all of the patients with FCD II except for one (Table 1), similar to that previously shown (53, 54). Surgical outcome was assessed using Engel's classification (45). Three out of eight individuals (38%) with FCD I had worse surgical outcome (class III or IV) compared to all seven individuals (100%) with FCD II (class I or II). Furthermore, the epilepsy control patients (n=4) who had an associated primary lesion such as a dysembryoplastic neuroepithelial tumor (DNET, WHO grade I), vascular malformation, or ganglioglioma but with no associated FCD had better surgical outcomes (class I or II). The improved surgical outcome in the patients with MRI lesions in this study is in agreement with previous studies (55). Based on review of the medical records, we also noted the presence of neurological conditions such as cognitive impairment, migraine, ADHD, depression, learning disabilities, and cerebral palsy in the study groups (Table 1).

Increased phospho-S6$^{240/244}$ staining in focal cortical dysplasia and tuberous sclerosis

We assessed mTOR signaling in the dysplastic tissue obtained from FCD I, FCD IIa, FCD IIb, and TS patients using immunostaining with anti-pS6$^{240/244}$ and anti-pS6$^{235/236}$ antibodies (Figures 2 and 3; respectively), which are considered markers of mTOR pathway

activation. Initially, we used the anti-pS6$^{240/244}$ antibody to confirm the previously reported mTORC1-dependent S6 phosphorylation in FCD II (35). No pS6$^{240/244}$ staining was visible in normal-appearing neurons from the non-dysplastic epilepsy control tissue (Figure 2A). Strong pS6$^{240/244}$ staining was visible in normal-sized dysmorphic neurons in tissue from all FCD I patients (Figure 2B) and in large dysmorphic neurons from all FCD IIa (Figure 2C), FCD IIb (Figure 2D), and TS patients (Figure 2F). Intense staining was also visible in the balloon cells in FCD IIb (Figure 2E) and giant cells in TS tissue (Figure 2G). The overall pS6$^{240/244}$ IHC score was significantly higher in FCD I ($n=8$, $p<0.001$) and FCD IIa ($n=3$, $p<0.05$) tissue as compared to control tissue (Figure 2H). Interestingly, although there were scattered foci of strong staining in FCD IIb tissue, the pS6$^{240/244}$ IHC score (calculated after multiplying immunostaining intensity by percentage of dysplastic brain parenchyma positive for the immunostaining) in FCD IIb tissue was not statistically different as compared to that in control tissue (Figure 2H). These data reveal increased phosphorylation levels of S6$^{240/244}$ suggesting mTOR pathway activation in FCD II and TS as previously shown by Baybis et al. (56). Furthermore, these results provide evidence of mTOR pathway activation in FCD I, which to our knowledge previously has not been reported.

Increased phospho-S6$^{235/236}$ staining in focal cortical dysplasia and tuberous sclerosis

Phosphorylation of S6 at S$^{235/236}$ also has been shown to be a marker of mTOR activation. Interestingly, both mTORC1 and ERK can phosphorylate S6 at S$^{235/236}$. In tissue stained with the anti-pS6$^{235/236}$ antibody, we found no staining in the normal appearing neurons from the non-dysplastic epilepsy control tissue, while relatively stronger pS6$^{235/236}$ staining was evident in normal-sized dysmorphic neurons localized in the dysplastic regions of FCD I (Figure 3B, 3F). In four of eight FCD I samples, there was variable pS6$^{235/236}$ staining in the normal-sized dysmorphic neurons (Figure 3B). This staining was not evident in the remaining four FCD I patients (data not shown). There was also stronger pS6$^{235/236}$ staining in the large dysmorphic neurons in FCD IIa (Figure 3C), FCD IIb (Figure 3D), and TS tissue (Figure 3F). There was relatively low pS6$^{235/236}$ staining in the balloon cells in FCD IIb (Figure 3E) and the giant cells in TS (Figure 3G). These findings suggest that S6 phosphorylation in morphologically abnormal cells observed in FCD could occur as mTORC1-dependent or -independent events with the latter potentially occurring through activation of the ERK pathway. Since variable amounts of pS6$^{235/236}$ staining were evident in the FCD I, there was no significant difference in the overall pS6$^{235/236}$ IHC score in the FCD I tissue as compared to control tissue (Figure 3H). In contrast, the pS6$^{235/236}$ IHC score was significantly higher in FCD IIa ($n=3$, $p<0.01$) and FCD IIb ($n=4$, $p<0.01$) tissue compared to that of controls ($n=4$; Figure 3H). Interestingly, the pS6$^{235/236}$ IHC score for FCD IIb was significantly higher compared to that for FCD I tissue ($n=8$; Figure 3H $p<0.05$, In comparison, the IHC score for FCD IIa tissue was not significantly elevated relative to FCD I tissue (Figure 3H).

TSC2 phosphorylation in focal cortical dysplasia II and tuberous sclerosis

We investigated phosphorylation of TSC2 (pTSC2) at the ERK regulatory site. TSC2 is phosphorylated by ERK at S^{664}, which then can lead to mTORC1 activation and increased pS6$^{240/244}$ levels (33). Immunohistochemistry was performed using the anti-pTSC2 antibody. We found no pTSC2 staining in the normal appearing neurons (Figure 4A) of the

non-dysplastic epilepsy control tissue. Similarly, the normal-sized dysmorphic neurons of FCD I tissue showed no pTSC2 staining (Figure 4B). Large dysmorphic neurons in one of the three cases of FCD IIa showed no pTSC2 staining (Figure 4C). However, the two other cases of FCD IIa showed diffuse pTSC2 staining in the large dysmorphic neurons (Figure 4D). Interestingly, diffusepTSC2 staining was observed in the large dysmorphic neurons in all of the FCD IIb (Figure 4E) and TS tissues (Figure 4G) that were included in this study. Balloon cells in the FCD IIb (Figure 4F) and the giant cells in TS (Figure 4H) also showed relatively strong staining for $pTSC2^{664}$. Furthermore, the overall pTSC2 IHC score was significantly higher in FCD IIb (n=4) tissue as compared to that in control (n=4, $p<0.05$) and FCD I (n=8, $p<0.01$; Figure 4I) tissue. Due to variable pTSC2 immunostaining in the FCD IIa tissue, there was no significant difference in the pTSC2 IHC score in control, FCD I, and FCD IIa tissue (Figure 4I).

Increased ERK pathway activation in focal cortical dysplasia II and tuberous sclerosis

Given the above findings showing increased phosphorylation of the ERK targets, S6 and TSC2, we stained FCD and TS tissue with the anti-pERK antibody, which recognizes ERK1/2 in its activated, dually phosphorylated state. We found no pERK staining in the non-dysplastic epilepsy control tissue (Figure 5A). There was no pERK staining in the normal sized dysmorphic neurons of FCD I. Interestingly, there was increased pERK staining in the astrocytic appearing cells of the dysplastic FCD I (Figure 5B) and FCD IIb tissue (Figure 5D). There was no appreciable staining in the large dysmorphic neurons in FCD IIa (Figure 5C). However, we found relatively strong pERK immunoreactivity in the balloon cells in FCD IIb (Figure 5E) and giant cells in TS tissue (Figure 5G). These findings suggest the presence of ERK activation in the balloon cells of FCD IIb and the giant cells in TS as well as astrocytes in FCD I and FCD IIb. The overall pERK IHC score was significantly higher in FCD IIb (n=4) as compared to FCD I (n=8, $p<0.001$), FCD IIa (n= 3, $p<0.001$), and control tissue (n=4, $p<0.0001$, Figure 5H). There was no statistical difference between FCD I, FCD IIa, and control tissue (Figure 5H).

DISCUSSION

Dysregulation of the mTOR pathway has been linked to malformations of cortical development (1, 2, 4, 18, 48, 57–60). Gene mutations in the upstream regulators of the mTOR pathway are associated with cortical deformities and epilepsy along with cognitive delay, behavioral disorders, and autism (13, 61, 62). Our findings using markers for mTORC1 activation in human brain tissue with FCD, further support mTOR pathway dysregulation in malformations of cortical development.

Staining with antibodies against $pS6^{235/236}$ and $pS6^{240/244}$, two biomarkers for activation of the mTOR pathway, revealed increased pS6 immunoreactivity in dysmorphic neurons from FCD I, FCD IIa and IIb, and TS tissue specimens. The IHC score for $pS6^{235/236}$ was statistically different in FCD I tissue as compared to FCD II, with FCD II tissue showing a higher score. In contrast, the IHC score for $pS6^{240/244}$ was not significantly different in the FCD I compared to the FCD II tissue. These findings suggest differential regulation of S6 phosphorylation at the $S^{235/236}$ sites in FCD I compared to FCD II. Furthermore, these

findings provide evidence for mTOR pathway activation in FCD I as well as FCD II. Additionally, in our study, $pS6^{235/236}$ staining was evident in the normal-sized dysmorphic neurons of four of eight FCD I patients, while $pS6^{240/244}$ staining was present in the normal-sized dysmorphic neurons in all the FCD I patients evaluated in this series. These novel findings are in contrast to that previously published by Crino et al. showing that mTOR is only activated in FCD II and not in FCD I (63). The reasons for this discrepancy may be related to variability in the levels of $pS6^{235/236}$ in FCD I as well as differences in the type of antibodies, staining techniques, duration of fixation, and type of antigen retrieval methods used. The difference in $pS6^{235/236}$ and $pS6^{240/244}$ staining in FCD I tissue might be due to changes in conformation of the ribosomal protein S6 based on the amount of phosphorylation of $S^{240/244}$, rendering the $S^{235/236}$ site accessible for phospho-regulation by ERK or S6K1. Additionally, our study showed both $pS6^{235/236}$ and $pS6^{240/244}$ antibody staining in the balloon cells in FCD IIb and the giant cells in TS. In support of our findings, Ljungberg et al. (50) have shown increased staining with the $pS6^{240/244}$ antibody and other downstream targets of the mTOR pathway such as phospho-eIF4G in large dysmorphic neurons and balloon cells of FCD II (7, 16). Animal models with mutations in upstream negative regulators of the mTOR pathway such as phosphatase tensin homolog (PTEN) (64–66) and tuberous sclerosis complex 1 and 2 (TSC1 and TSC2) (45, 58, 59) exhibit cortical dysplasia and severe epilepsy. Additionally, germline and more recently somatic mutations have been shown to be associated with malformation of cortical development including FCD (8, 12, 67–72).

ERK phosphorylation of TSC2 at S^{664} has been proposed as a mechanism for the loss of heterozygosity in TS, leading to activation of the mTOR pathway (38, 43, 44). Even though this mechanism has been described in TS, it has not been investigated in FCD. We investigated phosphorylation of TSC2 by ERK in FCD using an antibody that recognizes TSC2 when phosphorylated at serine 664, the ERK regulatory site. We found pTSC2 staining in the balloon cells of FCD IIb and giant cells of TS. In these cell types, we also detected increased levels of activated, dually phosphorylated ERK. The IHC score for pERK staining was significantly increased in FCD IIb tissue as compared to FCD I and FCD IIa. Similarly, the IHC score for pTSC2 staining was significantly higher in FCD IIb tissue as compared to FCD I and there was increased pTSC2 staining specifically in the balloon cells of FCD IIb where increased pERK immunostaining also was evident. In contrast, the positive pTSC2 immunostaining was not associated with pERK immunostaining in the large dysmorphic neurons of FCD IIa tissue. This observed difference might be due to transient ERK activation leading to constitutive TSC2 phosphorylation in large dysmorphic neurons of FCD IIb and TS. Further studies are necessary to further investigate this possibility.

Together, these findings further support aberrant mTOR pathway activation in FCD. In addition, our findings in FCD II reveal abnormal signaling in both the ERK and mTORC1 pathways, which in some aspects parallel the abnormal pathway activation that seen in TS. In contrast, we report evidence of mTORC1 hyperactivity in FCD I without evidence of ERK dysregulation at the level of TSC2. The positive immunostaining of pTSC2 in FCDII could be considered an indicator of the type of FCD pathology and possibly also the duration of epilepsy. This observation also supports the concept proposed by Crino et al. (1) that different types of FCD may represent a spectrum disorder, including isolated FCD

subtypes, TS, and hemimegalencephaly. mTOR pathway inhibitor treatment of humans with TS led to an overall decrease in seizure frequency (73). Taken together with our results, this clinical study supports the possibility of using mTOR inhibitors in other malformations of cortical development such as FCD. Furthermore, there may be a role for using ERK inhibitors as well in FCD II. Additional studies are warranted to further explore these concepts and the pathogenesis of FCD as well as the significance of ERK and mTOR pathways dysregulation in this disorder.

Acknowledgments

We would like to thank Dr. Cecilia Ljungberg for her intellectual contributions to this work and paper. This study was supported by the National Institutes of Health/National Institute for Neurological Disorders and Stroke (NIH/NINDS) R01 NS39943; R01 NS49427 (AEA); Vivian L Smith Foundation grant (AEA), and Epilepsy Foundation Predoctoral Fellowship (VVP). It also was supported by the BCM Intellectual and Developmental Disabilities Research Center (IDDRC) grant P30 HD024064 from the Eunice Kennedy Shriver National Institute of Child Health & Human Development. The content is solely the responsibility of the authors and does not necessarily represent the official views of the Eunice Kennedy Shriver National Institute of Child Health & Human Development or the NIH. The funders had no role in study design, data collection and analysis, decision to publish, or preparation of the manuscript.

References

1. Crino PB. Focal brain malformations: a spectrum of disorders along the mTOR cascade. Novartis Found Symp. 2007; 288:260–72. discussion 72–81. [PubMed: 18494264]
2. Wong M. Animal models of focal cortical dysplasia and tuberous sclerosis complex: recent progress toward clinical applications. Epilepsia. 2009; 50(Suppl 9):34–44.
3. Gleeson JG. Neuronal migration disorders. Ment Retard Dev Disabil Res Rev. 2001; 7(3):167–71. [PubMed: 11553932]
4. Lee JH, Huynh M, Silhavy JL, Kim S, Dixon-Salazar T, Heiberg A, et al. De novo somatic mutations in components of the PI3-AKT3-mTOR pathway cause hemimegalencephaly. Nat Genet. 2012; 44(8):941–45. [PubMed: 22729223]
5. Sisodiya SM, Fauser S, Cross JH, Thom M, Sisodiya SM, Fauser SM, et al. Focal cortical dysplasia type II: biological features and clinical perspectives. Lancet Neurol. 2009; 8(9):830–43. [PubMed: 19679275]
6. Palmini A, Najm I, Avanzini G, Babb T, Guerrini R, Foldvary-Schaefer N, et al. Terminology and classification of the cortical dysplasias. Neurology. 2004; 62(6 Suppl 3):S2–8.
7. Muhlebner A, Coras R, Kobow K, Feucht M, Czech T, Stefan H, et al. Neuropathologic measurements in focal cortical dysplasias: validation of the ILAE 2011 classification system and diagnostic implications for MRI. Acta neuropathologica. 2012; 123(2):259–72. [PubMed: 22120580]
8. Baulac S, Ishida S, Marsan E, Miquel C, Biraben A, Nguyen DK, et al. Familial focal epilepsy with focal cortical dysplasia due to DEPDC5 mutations. Annals of neurology. 2015; 77(4):675–83. [PubMed: 25623524]
9. Sarnat HB, Flores-Sarnat L. Infantile tauopathies: Hemimegalencephaly; tuberous sclerosis complex; focal cortical dysplasia 2; ganglioglioma. Brain Dev. 2014
10. Conti V, Pantaleo M, Barba C, Baroni G, Mei D, Buccoliero AM, et al. Focal dysplasia of the cerebral cortex and infantile spasms associated with somatic 1q21.1–q44 duplication including the AKT3 gene. Clin Genet. 2014
11. Mirzaa GM, Dobyns WB. The “megalencephaly-capillary malformation” (MCAP) syndrome: the nomenclature of a highly recognizable multiple congenital anomaly syndrome. Am J Med Genet A. 2013; 161A(8):2115–6. [PubMed: 23798482]
12. Lim JS, Kim WI, Kang HC, Kim SH, Park AH, Park EK, et al. Brain somatic mutations in MTOR cause focal cortical dysplasia type II leading to intractable epilepsy. Nat Med. 2015; 21(4):395–400. [PubMed: 25799227]

13. Crino PB. mTOR: A pathogenic signaling pathway in developmental brain malformations. Trends Mol Med. 2011; 17(12):734–42. [PubMed: 21890410]
14. Hay N, Sonenberg N. Upstream and downstream of mTOR. Genes & development. 2004; 18(16): 1926–45. [PubMed: 15314020]
15. Inoki K, Corradetti MN, Guan KL. Dysregulation of the TSC-mTOR pathway in human disease. Nat Genet. 2005; 37(1):19–24. [PubMed: 15624019]
16. Lin YX, Lin K, Kang DZ, Liu XX, Wang XF, Zheng SF, et al. Similar PDK1-AKT-mTOR pathway activation in balloon cells and dysmorphic neurons of type II focal cortical dysplasia with refractory epilepsy. Epilepsy Res. 2015; 112:137–49. [PubMed: 25847349]
17. Mori SNS, Kimura H, Tajima S, Takahashi Y, Kitamura A, Oneyama C, et al. The mTOR Pathway Controls Cell Proliferation by Regulating the FoxO3a Transcription Factor via SGK1 Kinase. PloS One. 2014; 9(2):e88891. [PubMed: 24558442]
18. Sarbassov DD, Ali SM, Sabatini DM. Growing roles for the mTOR pathway. Current opinion in cell biology. 2005; 17(6):596–603. [PubMed: 16226444]
19. Bateup HS, Johnson CA, Denefrio CL, Saulnier JL, Kornacker K, Sabatini BL. Excitatory/inhibitory synaptic imbalance leads to hippocampal hyperexcitability in mouse models of tuberous sclerosis. Neuron. 2013; 78(3):510–22. [PubMed: 23664616]
20. Li Y, Meloni EG, Carlezon WA, Milad MR, Pitman RK, Nader K, et al. Learning and reconsolidation implicate different synaptic mechanisms. Proc Natl Acad Sci USA. 2013; 110(12): 4798–803. [PubMed: 23487762]
21. Cloëtta D, Thomanetz V, Baranek C, Lustenberger RM, Lin S, Oliveri F, et al. Inactivation of mTORC1 in the developing brain causes microcephaly and affects gliogenesis. J Neurosci. 33(18): 7799–810.
22. McMahon J, Huang X, Yang J, Komatsu M, Yue Z, Qian J, et al. Impaired autophagy in neurons after disinhibition of mammalian target of rapamycin and its contribution to epileptogenesis. J Neurosci. 2012; 32(45):15704–14. [PubMed: 23136410]
23. Tang Z, Berezcki E, Zhang H, Wang S, Li C, Ji X, et al. Mammalian target of rapamycin (mTor) mediates tau protein dyshomeostasis: implication for Alzheimer disease. J Biol Chem. 2013; 288(22):15556–70. [PubMed: 23585566]
24. Bowling H, Klann E. Shaping dendritic spines in autism spectrum disorder: mTORC1-dependent macroautophagy. Neuron. 2014; 83(5):994–6. [PubMed: 25189205]
25. Kim YT, Hur EM, Snider WD, Zhou FQ. Role of GSK3 Signaling in Neuronal Morphogenesis. Front Mol Neurosci. 2011; 4:48. [PubMed: 22131966]
26. Malagelada C, Lopez-Toledano MA, Willett RT, Jin ZH, Shelanski ML, Greene LA. RTP801/REDD1 regulates the timing of cortical neurogenesis and neuron migration. J Neurosci. 2011; 31(9):3186–96. [PubMed: 21368030]
27. Feliciano DM, Bordey A. Newborn cortical neurons: only for neonates? Trends Neurosci. 2013; 36(1):51–61. [PubMed: 23062965]
28. Gao X, Zhang Y, Arrazola P, Hino O, Kobayashi T, Yeung RS, et al. Tsc tumour suppressor proteins antagonize amino-acid-TOR signalling. Nat Cell Biol. 2002; 4(9):699–704. [PubMed: 12172555]
29. Inoki K, Li Y, Zhu T, Wu J, Guan KL. TSC2 is phosphorylated and inhibited by Akt and suppresses mTOR signalling. Nature cell biology. 2002; 4(9):648–57. [PubMed: 12172553]
30. Tee AR, Manning BD, Roux PP, Cantley LC, Blenis J. Tuberous sclerosis complex gene products, Tuberin and Hamartin, control mTOR signaling by acting as a GTPase-activating protein complex toward Rheb. Current biology: CB. 2003; 13(15):1259–68. [PubMed: 12906785]
31. Kim DH, Sarbassov DD, Ali SM, King JE, Latek RR, Erdjument-Bromage H, et al. mTOR interacts with raptor to form a nutrient-sensitive complex that signals to the cell growth machinery. Cell. 2002; 110(2):163–75. [PubMed: 12150925]
32. Kim DH, Sarbassov DD, Ali SM, Latek RR, Guntur KVP, et al. GbetaL, a positive regulator of the rapamycin-sensitive pathway required for the nutrient-sensitive interaction between raptor and mTOR. Molecular cell. 2003; 11(4):895–904. [PubMed: 12718876]
33. Wullschleger S, Loewith R, Hall MN. TOR signaling in growth and metabolism. Cell. 2006; 124(3):471–84. [PubMed: 16469695]

34. Gao X, Pan D. TSC1 and TSC2 tumor suppressors antagonize insulin signaling in cell growth. Genes Dev. 2001; 15(11):1383–92. [PubMed: 11390358]
35. Pende M, Um SH, Mieulet V, Sticker M, Goss VL, Mestan J, et al. S6K1(−/−)/S6K2(−/−) mice exhibit perinatal lethality and rapamycin-sensitive 5′-terminal oligopyrimidine mRNA translation and reveal a mitogen-activated protein kinase-dependent S6 kinase pathway. Mol Cell Biol. 2004; 24(8):3112–24. [PubMed: 15060135]
36. Yue Q, Groszer M, Gil JS, Berk AJ, Messing A, Wu H, et al. PTEN deletion in Bergmann glia leads to premature differentiation and affects laminar organization. Development. 2005; 132(14): 3281–91. [PubMed: 15944184]
37. Kwiatkowski DJ. Tuberous sclerosis: from tubers to mTOR. Ann Hum Genet. 2003; 67(Pt 1):87–96. [PubMed: 12556239]
38. Ma L, Chen Z, Erdjument-Bromage H, Tempst P, Pandolfi PP. Phosphorylation and functional inactivation of TSC2 by Erk implications for tuberous sclerosis and cancer pathogenesis. Cell. 2005; 121(2):179–93. [PubMed: 15851026]
39. Kumar V, Zhang MX, Swank MW, Kunz J, Wu GY. Regulation of dendritic morphogenesis by Ras-PI3K-Akt-mTOR and Ras-MAPK signaling pathways. J Neurosci. 2005; 25(49):11288–99. [PubMed: 16339024]
40. Okuyama N, Takagi N, Kawai T, Miyake-Takagi K, Takeo S. Phosphorylation of extracellular-regulating kinase in NMDA receptor antagonist-induced newly generated neurons in the adult rat dentate gyrus. J Neurochem. 2003; 88(3):717–25.
41. Peng S, Zhang Y, Zhang J, Wang H, Ren B. ERK in learning and memory: A review of recent research. Int J Mol Sci. 2010; 11(1):222–32. [PubMed: 20162012]
42. Zhang L, Bartley CM, Gong X, Hsieh LS, Lin TV, Feliciano DM, et al. MEK-ERK1/2-dependent FLNA overexpression promotes abnormal dendritic patterning in tuberous sclerosis independent of mTOR. Neuron. 2014; 84(1):78–91. [PubMed: 25277454]
43. Govindarajan B, Mizesko MC, Miller MS, Onda H, Nunnelley M, Casper K, et al. Tuberous sclerosis-associated neoplasms express activated p42/44 mitogen-activated protein (MAP) kinase, and inhibition of MAP kinase signaling results in decreased in vivo tumor growth. Clin Cancer Res. 2003; 9(9):3469–75. [PubMed: 12960139]
44. Jozwiak J, Grajkowska W, Kotulska K, Jozwiak S, Zalewski W, Zajaczkowska A, et al. Brain tumor formation in tuberous sclerosis depends on Erk activation. Neuromolecular Med. 2007; 9(2):117–27. [PubMed: 17627032]
45. Tonini C, Beghi E, Berg AT, Bogliun G, Giordano L, Newton RW, et al. Predictors of epilepsy surgery outcome: a meta-analysis. Epilepsy Res. 2004; 62(1):75–87. [PubMed: 15519134]
46. Crino PB. Malformations of cortical development: molecular pathogenesis and experimental strategies. Adv Exp Med Biol. 2004; 548:175–91. [PubMed: 15250594]
47. Crino PB. Molecular pathogenesis of tuber formation in tuberous sclerosis complex. J Child Neurol. 2004; 19(9):716–25. [PubMed: 15563019]
48. Crino PB, Nathanson KL, Henske EP. The tuberous sclerosis complex. The New England journal of medicine. 2006; 355(13):1345–56. [PubMed: 17005952]
49. Inoki K, Li Y, Xu T, Guan KL. Rheb GTPase is a direct target of TSC2 GAP activity and regulates mTOR signaling. Genes & development. 2003; 17(734):1829–34. [PubMed: 12869586]
50. Ljungberg MC, Bhattacharjee MB, Lu Y, Armstrong DL, Yoshor D, Swann JW, et al. Activation of mammalian target of rapamycin in cytomegalic neurons of human cortical dysplasia. Annals of neurology. 2006; 60(4):420–9. [PubMed: 16912980]
51. McCarty KS Jr, Szabo E, Flowers JL, Cox EB, Leight GS, Miller L, et al. Use of a monoclonal anti-estrogen receptor antibody in the immunohistochemical evaluation of human tumors. Cancer Res. 1986; 46(8 Suppl):4244s–8s. [PubMed: 3524805]
52. Blumcke I, Muhlebner A. Neuropathological work-up of focal cortical dysplasias using the new ILAE consensus classification system - practical guideline article invited by the Euro-CNS Research Committee. Clin Neuropathol. 2011; 30(4):164–77. [PubMed: 21726501]
53. Kim DW, Kim S, Park SH, Chung CK, Lee SK. Comparison of MRI features and surgical outcome among the subtypes of focal cortical dysplasia. Seizure. 2012; 21(10):789–94. [PubMed: 23040369]

54. Tassi L, Garbelli R, Colombo N, Bramerio M, Russo GL, Mai R, et al. Electroclinical, MRI and surgical outcomes in 100 epileptic patients with type II FCD. Epileptic Disord. 2012; 14(3):257–66. [PubMed: 22963868]
55. Tassi L, Colombo N, Garbelli R, Francione S, Lo Russo G, Mai R, et al. Focal cortical dysplasia: neuropathological subtypes, EEG, neuroimaging and surgical outcome. Brain. 2002; 125(8):1719–32. [PubMed: 12135964]
56. Baybis M, Yu J, Lee A, Golden JA, Weiner H, McKhann G 2nd, et al. mTOR cascade activation distinguishes tubers from focal cortical dysplasia. Annals of neurology. 2004; 56(4):478–87. [PubMed: 15455405]
57. Crino PB. Gene expression, genetics, and genomics in epilepsy: some answers, more questions. Epilepsia. 2007; 48(Suppl 2):42–50.
58. Mathern GW. Epilepsy surgery patients with cortical dysplasia: present and future therapeutic challenges. Neurology. 2009; 72(3):206–7. [PubMed: 19005172]
59. Mathern GW. Challenges in the surgical treatment of epilepsy patients with cortical dysplasia. Epilepsia. 2009; 50(Suppl 9):45–50.
60. Sarbassov DD, Guertin DA, Ali SM, Sabatini DM. Phosphorylation and regulation of Akt/PKB by the rictor-mTOR complex. Science. 2005; 307(5712):1098–101. [PubMed: 15718470]
61. Lasarge CL, Danzer SC. Mechanisms regulating neuronal excitability and seizure development following mTOR pathway hyperactivation. Front Mol Neurosci. 2014; 7(18) eCollection 2014.
62. Napolioni V, Curatolo P. Genetics and molecular biology of tuberous sclerosis complex. Curr Genomics. 2008; 9(7):475–87. [PubMed: 19506736]
63. Lim KC, Crino PB. Focal malformations of cortical development: new vistas for molecular pathogenesis. Neuroscience. 2013; (252):262–76. IBRO.
64. Backman A, Stambolic V, Suzuki A, Haight J, Elia A, Pretorius J, et al. Deletion of Pten in mouse brain causes seizures, ataxia and defects in soma size resembling Lhermitte-Duclos disease. Nat Genet. 2001; 29(4):396–403. [PubMed: 11726926]
65. Kwon CH, Zhu X, Zhang J, Knoop LL, Tharp R, Smeyne RJ, et al. Pten regulates neuronal soma size: a mouse model of Lhermitte-Duclos disease. Nat Genet. 2001; 29(4):404–11. [PubMed: 11726927]
66. Ogawa S, Kwon CH, Zhou J, Koovakkattu D, Parada LF, Sinton CM. A seizure-prone phenotype is associated with altered free-running rhythm in Pten mutant mice. Brain Res. 2007; 1168:112–23. [PubMed: 17706614]
67. Costa-Mattioli M, Sossin WS, Klann E, Sonenberg N. Review Translational Control of Long-Lasting Synaptic Plasticity and Memory. Neuron. 2009; 61(1):10–26. [PubMed: 19146809]
68. Ehninger D, Han S, Shilyansky C, Zhou Y, Li W, Kwiatkowski DJ, et al. Reversal of learning deficits in a Tsc2+/− mouse model of tuberous sclerosis. Nat Med. 2008; 14(8):843–8. [PubMed: 18568033]
69. Kwon CH, Zhou J, Li Y, Kim KW, Hensley LL, Baker SJ, et al. Neuron-specific enolase-cre mouse line with cre activity in specific neuronal populations. Genesis. 2006; 44(3):130–5. [PubMed: 16496331]
70. Richter JD, Klann E. Making synaptic plasticity and memory last/: mechanisms of translational regulation. Genes & development. 2009; 23(1):1–11. [PubMed: 19136621]
71. Talos DM, Kwiatkowski DJ, Cordero K, Black PM, Jensen FE. Cell-specific alterations of glutamate receptor expression in tuberous sclerosis complex cortical tubers. Annals of neurology. 2008; 63(4):454–65. [PubMed: 18350576]
72. Zhou J, Blundell J, Ogawa S, Kwon CH, Zhang W, Sinton C, et al. Pharmacological inhibition of mTORC1 suppresses anatomical, cellular, and behavioral abnormalities in neural-specific Pten knock-out mice. J Neurosci. 2009; 29(6):1773–83. [PubMed: 19211884]
73. Curatolo P. Mechanistic target of rapamycin (mTOR) in tuberous sclerosis complex-associated epilepsy. Pediatr Neurol. 2015; 52(3):281–9. [PubMed: 25591831]

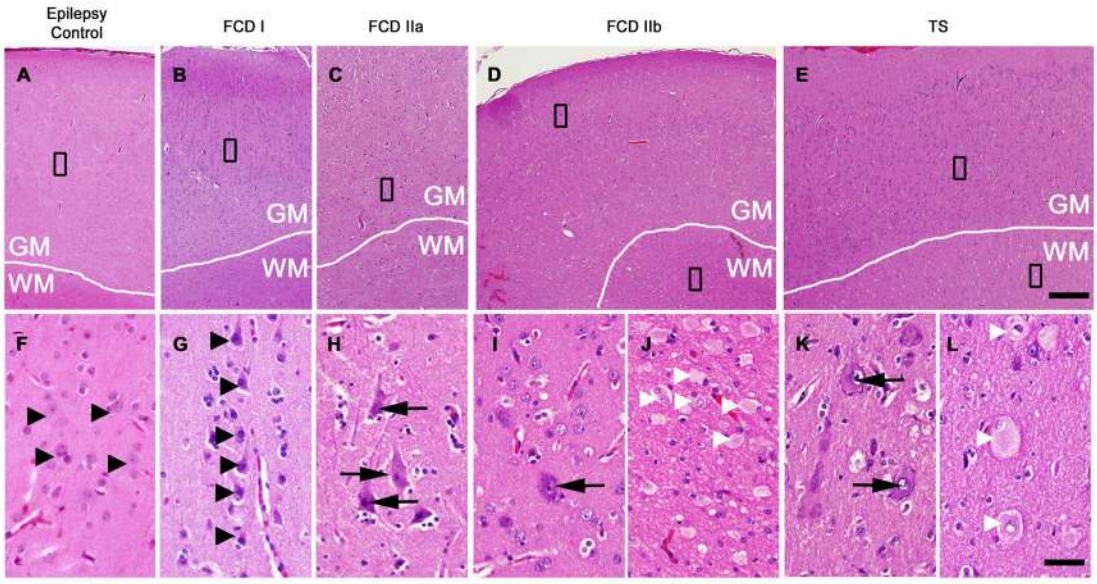

Figure 1.

Histological appearance of representative focal cortical dysplasia type I (FCD I), type IIa (FCD IIa), type IIb (FCD IIb) and tuberous sclerosis (TS) tissue with hematoxylin and eosin staining. Panels A – E show low magnification photomicrographs and panels F – L show high magnification photomicrographs of the area outlined by black box in the low magnification pictures. Epilepsy control tissue is shown with normal appearing neurons (A; F, black arrowheads) in the gray matter used for comparison. FCD I tissue (B) shows the presence of vertical columns of normal-sized dysmorphic neurons (G, black arrowheads). FCD IIa (C), FCD IIb (D) and TS (E) tissue is shown with disoriented and abnormally large dysmorphic neurons (H, I and K, black arrows). FCD IIb and TS show eosinophilic balloon cells and giant cells (J and L, white arrowheads) mainly in white matter in addition to large dysmorphic neurons (I and K, black arrows) mainly in gray matter. Scale bar (A – E) = 500 μm and (F – L) = 50 μm.

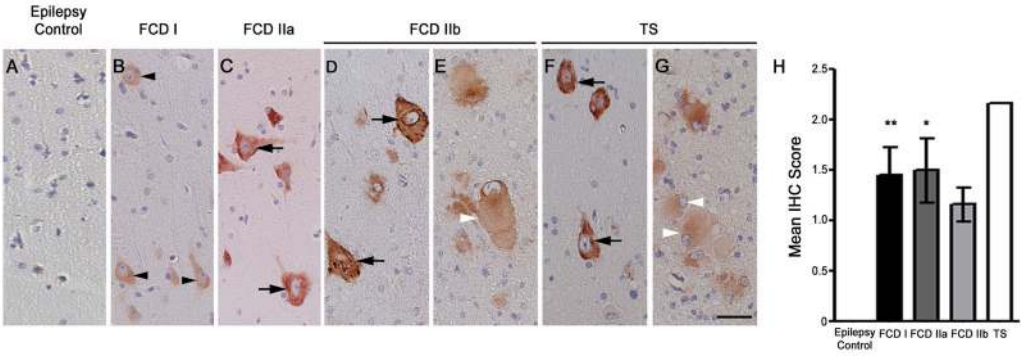

Figure 2.

Increased ribosomal S6 phosphorylation at $S^{240/S244}$ in focal cortical dysplasia (FCD) and tuberous sclerosis (TS). Normal appearing neurons in epilepsy control (A) cortices are used for comparison and are negative for $pS6^{240/244}$ staining. Normal-sized dysmorphic neurons (black arrowheads) in FCD I (B) are weakly immunoreactive for phospho-S6 ($pS6^{240/244}$). Large dysmorphic neurons (black arrows) in FCD IIa (C), IIb (D), and TS (F) are strongly immunoreactive, while balloon cells (E, white arrowheads) in FCD IIb and giant cells in TS (G, white arrowheads) are immunoreactive for $pS6^{240/244}$. Scale bar = 50 μm. The overall $pS6^{240/244}$ IHC score was significantly higher in FCD I (n=8, $p<0.001$) and FCD IIa (n=3, $p<0.05$) tissue samples as compared to that in control samples (n=4; H). The $pS6^{240/244}$ IHC score in FCD IIb tissue samples (n=4) was not statistically different as compared to that of control tissue samples. The $pS6^{240/244}$ IHC score in TS (n=2) tissue was higher as compared to that of control tissue.

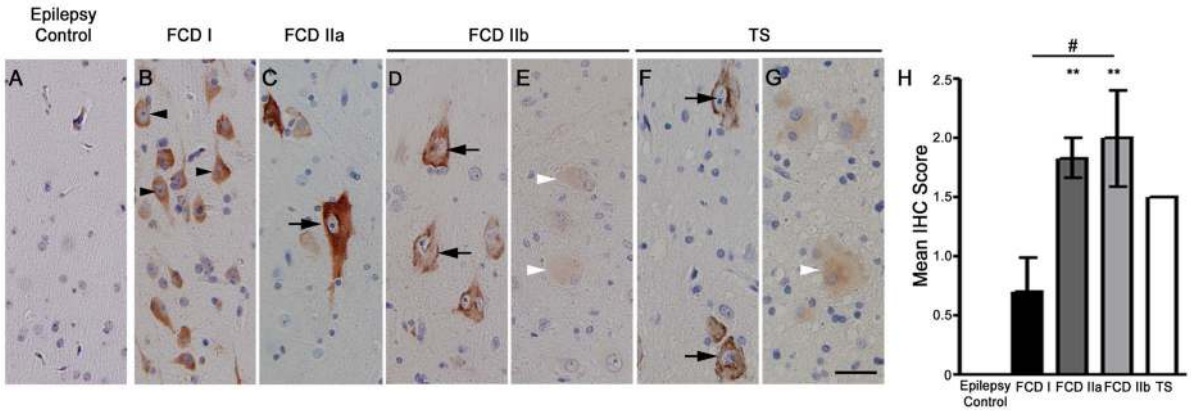

Figure 3.

Increased ribosomal S6 phosphorylation at $S^{235/S236}$ sites in focal cortical dysplasia (FCD) and tuberous sclerosis (TS). Normal appearing neurons (A) in epilepsy control cortices are used for comparison and are negative for $pS6^{235/236}$ staining. Normal-sized dysmorphic neurons (black arrowheads) in FCD I (B) are strongly immunoreactive for phospho-S6 ($pS6^{235/236}$). Large dysmorphic neurons (black arrows) in FCD IIa (C), IIb (D), and TS (F) are strongly immunoreactive for $pS6^{235/236}$. On the contrary, balloon cells (E, white arrowheads) in FCD IIb and giant cells (G, white arrowheads) in TS are weakly immunoreactive for $pS6^{235/236}$. Scale bar = 50 μm. The overall $pS6^{235/236}$ IHC score in FCD IIa ($n=3$, $p<0.01$) and FCD IIb ($n=4$, $p<0.01$) tissue samples was significantly higher than that of the control tissue ($n=4$; H). The $pS6^{235/236}$ IHC score in FCD IIb ($n=4$, $p<0.05$) tissue was significantly higher as compared to that in FCD I tissue samples ($n=8$; B). The $pS6^{235/236}$ IHC score in FCD I tissue samples ($n=8$; H) was not significantly different from that of controls.

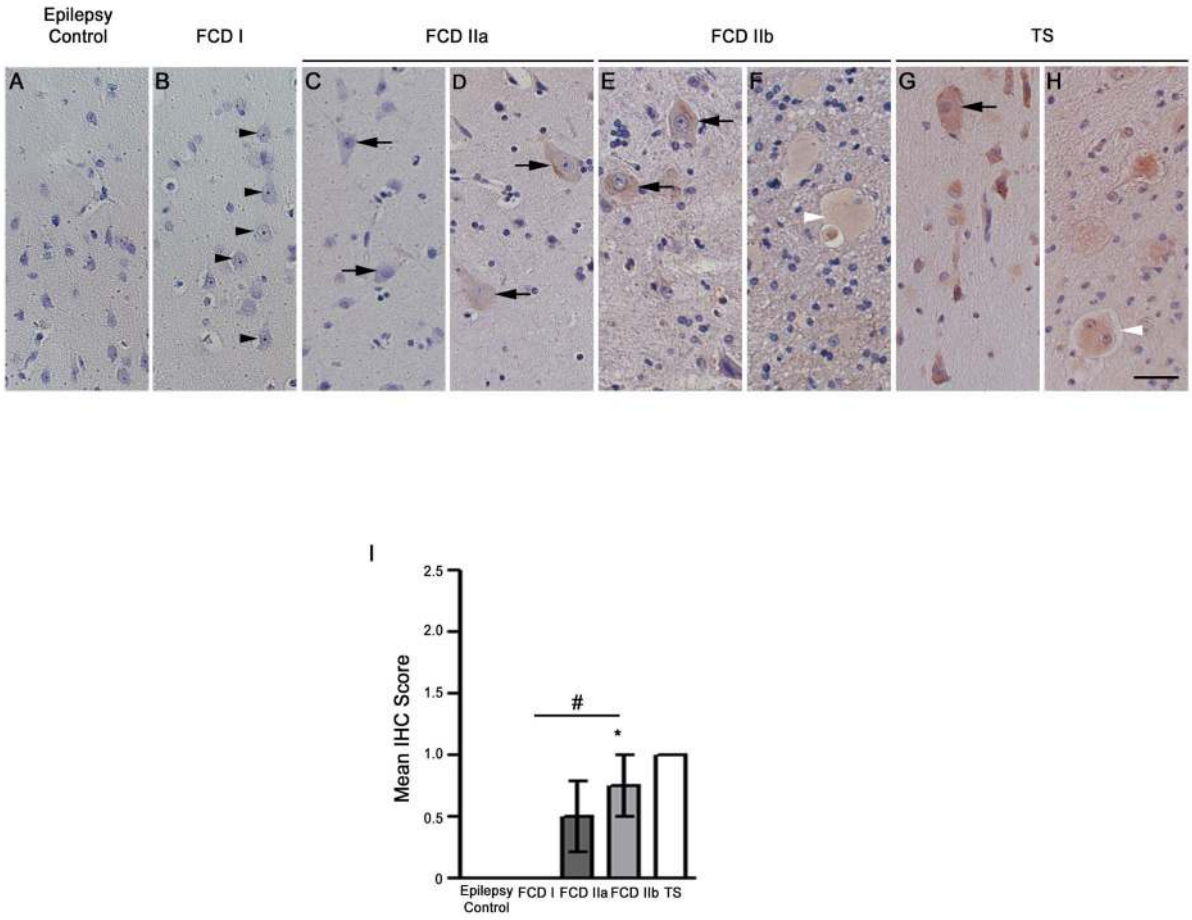

Figure 4.

Increased tuberous sclerosis complex 2 (TSC2) phosphorylation at S^{664} in focal cortical dysplasia II (FCD II) and tuberous sclerosis (TS). Normal appearing neurons (A) in epilepsy control cortices are shown for comparison and are negative for pTSC2 staining. Normal-sized dysmorphic neurons (B, black arrowheads) in FCD I do not stain for phospho-TSC2 (pTSC2). Large dysmorphic neurons (C, black arrows) are negative for pTSC2 in two FCD IIa patients, but are positive in one FCD IIa (D), all FCD IIb (E), and TS patients (G). Balloon cells (F, white arrowhead) in FCD IIb and giant cells (H, white arrowhead) in TS are also immunoreactive for pTSC2. Scale bar = 50 μm. The overall pTSC2 IHC score was significantly higher in FCD IIb tissue (n=4, $p<0.05$) as compared to that of controls (n=4; I). The pTSC2 IHC score was significantly higher in the FCD IIb (n=4, $p<0.01$; I) tissue samples as compared to that in FCD I (n=8) tissue samples. There was no statistical difference in the pTSC2 IHC scoring in FCD I (n=8) and FCD IIa (n=3) tissue samples as compared to control (n=4) tissue samples (I).

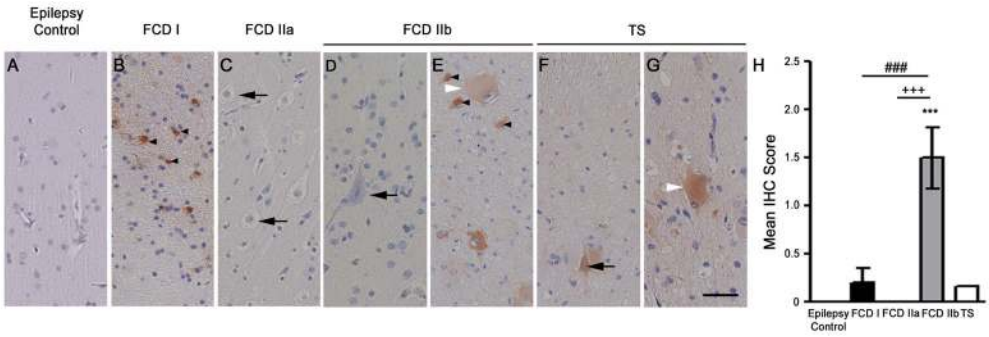

Figure 5.

Increased phosphorylation of extracellular regulated kinase (pERK) in focal cortical dysplasia (FCD) and tuberous sclerosis (TS). Normal appearing neurons (A) in epilepsy control cortices are shown for comparison and are negative for pERK staining. Numerous astrocytes close to the pial surface (data not shown) and in white matter of FCD I (B, black arrowheads), and FCD IIb (E) tissue stained strongly for pERK. Large dysmorphic neurons in FCD IIa (C, black arrows) and FCD IIb (D, black arrows) are negative for pERK, while both balloon cells (E, white arrowhead) in FCD IIb and giant cells (G, white arrowhead) in TS are immunoreactive for pERK. Normal-sized and large dysmorphic neurons (F, black arrows) are immunoreactive for pERK in TS. Scale bar = 50 μm. The overall pERK IHC score was significantly higher in FCD IIb (n=4) as compared to FCD I (n=8, $p<0.001$), FCD IIa (n= 3, $p<0.001$) and control tissue (n=4, $p<0.001$, H). Interestingly, there was no difference between pERK IHC score in control tissue samples as compare to that of TS tissue samples (n=2; H, statistical difference cannot be identified due to low tissue sample).

Table 1

Clinical features of the patients with cortical dysplasia and tuberous sclerosis

ADHD: attention deficit hyperkinetic disorder, OCD: obsessive-compulsive disorder, DNET: dysembryonic neuroepithetial tumor, and TS: tuberous sclerosis. The last five patients had non-dysplastic tissue associated with the resected tissue which served as epilepsy control tissue

Age (yrs)	Age of Onset (yrs)	Location (Lobe)	Type of focal cortical dysplasia	Associated medical conditions	MRI lesion	Surgical outcome
15	10.5	Right frontal	I	None	Not present	Class I
18	10	Right orbitofrontal	I	Mild mental retardation (IQ=80)	Not present	Class II
16	10.5	Right orbitofrontal, lateral temporal, temporal	I	Migraine with aura	Not present	Class III
6	5	Left lateral temporal cortex, hippocampus	I	None	Not present	Class IV
4	3	Right orbitofrontal	I	None	Not present	Class I
14	5	Right fronto-temporal lobe	I	Cognitive decline	Present	Class I
0.42	0.42	Left temporal	I	Global developmental delay, Microcephaly	Present	Class I
12	9	Right superior temporoparietal	I	ADHD	Not present	Class III
18	5	Left temporo-occipital	IIa	ADHD	Present	Class I
10	1	Left frontal	IIa	Mild global delay, Autism	Present	Class I
15	9	Right parietal	IIa	Depression	Present	Class II
13	4	Right frontal	IIb	None	Not present	Class I
11	6.5	Right frontal	IIb	OCD	Present	Class I
18	2	Left occipital	IIb	Learning difficulties, dyslexia	Present	Class I
15	0.5	Left frontoparietal	IIb	Mild Hemiperetic cerebral palsy	Present	Class II
1.5	0.34	Left temporoparietal	TS	TS	Present	Class III
6	2	Left frontal lobe	TS	TS, receptive and expressive language disorder, Autistic spectrum features	Present	Class I
13	6	Right temporal	Ganglioliomа	None	Present	Class I
9	5	Left temporal	DNET	Learning difficulties	Present	Class II
2	1	Right temporal	Leptomenin meal vascular malformation with transmantle CD	None	Present	Class I
5	5	Left temporo-occipital	Ganglioliomа	None	Present	Class I